Journal of Materials and Environmental Sciences
ISSN : 2028-2508
CODEN : JMESCN

J. Mater. Environ. Sci., 2019, Volume 10, Issue 6, Page 485-494

http://www.jmaterenvironsci.com

Parameters affecting the photodegradation rate of imidacloprid catalyzed by ZnO nanoparticles

Asmaa A. Atwan[1,3], Ibrahim M. Elmehasseb[1], N.I. Talha[3], Maged El-Kemary[2]

[1]*Chemistry Department, Faculty of Science, Kafrelsheikh University, 33516 Kafr ElSheikh, Egypt.*
[2]*Nanoscience & Nanotechnology Institute, Kafrelsheikh University, 33516 Kafr ElSheikh, Egypt.*
[3]*Soils, Waters and Environment Research Institute. ARC, Egypt.*

Received 8 May2019,
Revised 16 June 2019,
Accepted 18 June 2019

Keywords
- ✓ *Nanoparticles,*
- ✓ *ZnO,*
- ✓ *Ag-doped ZnO,*
- ✓ *Imidacloprid,*
- ✓ *Photodegradtion.*

Asmaa Atwan
jodikhairy@gmail.com

Abstract

Herein, a study of imidaclopridphotodegradation in water catalyzed by zinc oxide nanoparticles and some parameters affecting its rate of degradation like ZnO load, imidacloprid initial concentration, reaction temperature, initial pH of the solution and doping with 5% (w: w) silver. At first zinc oxide nanoparticles were prepared via a solvothermal method with an average diameter about 26.6 nm, then it is doped with silver by a photo-reduction method using silver nitrate and ethylene glycol in day light. The obtained samples were characterized by XRD, TEM, SEM, SEM/EDX, UV-VIS spectrum and FTIR. The imidacloprid degradation rate was monitored using UV-VIS spectrophotometer.

1. Introduction

Wastewater reuse for agriculture proposes is a practical solution to overcome shortage of water problem, especially in arid and semi arid regions [1]. However, Wastewater irrigation creates benefits like that it adds valuable nutrients and organic matter to soil and also provides a reliable irrigation water supply [2-6], it also has some risks if it applied without being treated adequately as it may represent possible sources of plant and soil contamination [2, 6-11]. One of the most dangerous wastewater pollutants is pesticides which have many sources like routine agricultural practice, wastewater from agricultural industry, rinse water and plant residues contaminated with pesticides [12], so various strategies have been relayed to produce more clean water sources [13]. Nowadays, Heterogeneous photocatalysis has the most of researches concern as it's an effective and promising technique for treatment of water in comparison to the other traditional methods [14] due to some features that it have like (a) it mineralizes the parent compounds and their intermediate without any secondary pollutant, (b) ambient operating temperature and pressure and (c) low cost of operation [10, 13, 15, 16].

The most important feature of any photo catalyst is its surface area. Nanocrystalline photocatalysts allow higher adsorption of the target as it offers a large surface to volume ratios [17]. In materials science, ZnO is categorized as a semiconductor in group II-VI, whose covalence is on the boundary between ionic and covalent semiconductors. It is regarded as an appealing semiconductor for potential use in electronics, optoelectronics and laser technology as it offers a broad energy band (3.37 eV), high bond energy (60 meV) and high thermal and mechanical stability at room temperature [18-20].

ZnO is an attractive material for water treatment as it can be tailored to absorb visible light and is capable of ushering in the era of solar photocatalysis. It has an edge over other metal oxides like TiO_2 in water purification and other environmental remediation processes as it is soluble in water and ends up as metallic zinc in the ecosystem [15, 20]. When a photon with an energy of hν matches or exceeds the band gap energy (Eg) of ZnO, an electron (e_{cb}^-) from the valence band (VB) is excited and enters to the conduction band (CB) leaving a hole (h_{vb}^+) behind [21,22], but those electrons of excited state conduction band and holes of valence band recombine rapidly which in turn leads to impede the redox reactions.

Modification of ZnO surface with noble metals doping can limit the recombination of electron hole pairs due to the formation of Schottky junction and subsequent redox reactions may occur, also can increase the broadness of its absorption spectrum [23-25]. Among the noble metals, silver has attracted much concern as a dopant as it is the cheapest one, possess good physical and chemical properties and high-efficiency metal-ZnO photocatalyst [26-33].
Neonicotinoid insecticides represent the most important chemical class of insecticides introduced to the global market since the synthetic pyrethroids [34]. Imidacloprid an example of this class is the most widely used insecticides in the world [35]. In this work undoped ZnO and Ag-doped ZnO NPs were prepared and characterized to study the imidacloprid photocatalytic degradation rate and the parameters affecting the degradation rate.

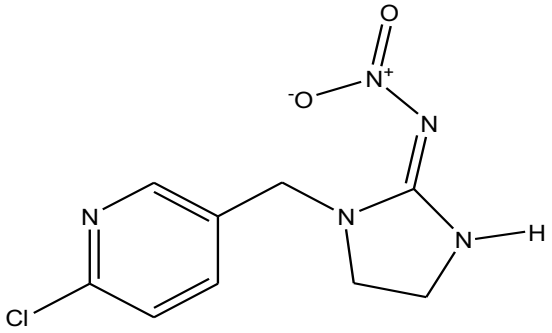

Imidacloprid chemical structure

2. Material and method

2.1. Chemicals

Zinc acetate dihydrate (Sigma Aldrich), Methanol (Local Market), Sodium hydroxide (AppliChem Panreac), Silver nitrate (Cambrian Chemicals), Ethylene glycol (NICE CHEMICALS), Imidacloprid (Jiangsu Fengshan Group Co., LTD – China).

2.2. Synthesis of ZnO NPs

A Stock solution of zinc acetate dihyderate (0.2 M) was prepared in 50 ml methanol under stirring, then to this solution 25 ml of sodium hydroxide (0.4 M) solution was added drop wise under continuous stirring. This solution was transferred into 100 ml Teflon lined sealed stainless steel autoclave and maintained at 60^{o}C for 6 hours under autogenous pressure. It was allowed to cool naturally at room temperature after the reaction was completed. The resulting milky solution is then centrifuged, washed with double distilled water, then ethanol and dried in a laboratory oven at 70^{o}C [36].

2.3. Ag-doped ZnO NPs synthesis

0.2 g ZnO was added to 6 ml ethylene glycol containing the desired amount of $AgNO_3$ about 5% (w: w) and then was stirred in dark to make a complete adsorption of Ag ions on the surface of ZnO then it is exposed to daylight until its color turns into brown then the solution was centrifuged, washed with double distilled water and ethanol and dried in an oven at 60^{o}C [37]. `

2.4. Characterization

The as prepared ZnO and Ag-doped ZnO nanoparticles (NPs) were characterized by X-ray diffraction (XRD) (Shimadzu XRD-6000), Transmission electron microscope (TEM) (JEOL JEM-2100), UV-VIS spectrophotometer (Shimadzu UV-2450), Scanning electron microscope (SEM) (JEOL JSM-IT100), SEM/EDX and FTIR (JASCO FT/IR-6800).

2.5. Photocatlytic degradation

Photodegradation of Imidaclporid pesticide using ZnO and Ag-doped ZnO NPs as catalysts have been measured under UV light at 365 nm. The degradation of Imidacloprid was followed by measuring the change in the absorption intensity at ($\lambda_{(max)}$=270 nm) using Shimadzu UV-VIS spectrophotometer versus interval times. All concentrations were prepared in double distilled water and the degradation rate (R%) was calculated with equation (1) as follows

$$R\% = \left[\frac{A_o - A}{A_o}\right] \times 100 \qquad (1)$$

Where A_o represents the initial absorbance of the target and A represents the absorbance after degradation for a given time (t).

3. Results & discussion

3.1. Characterization of materials.

Figure1 shows XRD patterns of ZnO and Ag-doped ZnO samples with about 5% (w: w) of silver. The intensity data were collected over a 2θ range of (10-80) with scan rate 8 min^{-1}. The two patterns peaks match well with the standard wurtizite structure of ZnO (JCPDS card no. 36-1451) while there were 3 additional peaks in Ag-doped ZnO pattern at 2θ of 37.51, 43.92 and 64.11 attributed to metallic Ag FCC phase (JCPDS card no. 04-0783) which indicates that crystalline silver clusters are clearly formed as a second phase. No any other crystal phase diffraction peaks were detected, indicating the purity of the samples. With Ag doping, the peaks position is shifted toward lower values indicating a partial substitution of Ag^+ ions at the ZnO lattice and this can be attributed to being Ag^+ ion (1.22Å) has higher ionic size than a Zn^{2+} ion (0.74Å) [38].The crystalline size of ZnO NPs was determined by using the Debye Scherer equation (2) as follows

$$D = \frac{k\lambda}{\beta.\cos\theta} \qquad (2)$$

Where D is the crystalline size in nanometers, λ =1.54 the X-ray wavelength, k is a constant equal 0.94, β is the peak width at half –maximum intensity, and θ is Bragg angle. The crystalline size of ZnO NPs in ZnO and Ag-doped ZnO samples at 2θ=35.8 is estimated as 29.7 and 31.1 nm respectively.

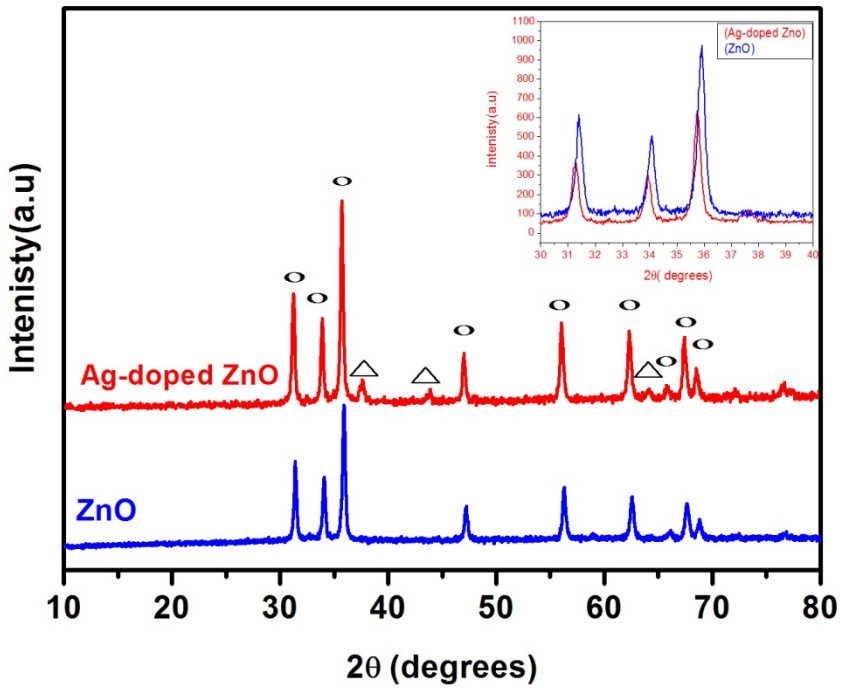

Figure 1: XRD pattern of (ZnO) and (Ag-doped ZnO) NPs.

For indicating the shape and size of ZnO and Ag-doped ZnO NPs the TEM images were used. ZnO and Ag-doped ZnO NPs were dispersed in anhydrous alcohol to prepare dilute suspension. Figure 2 shows the TEM images of ZnO and Ag-doped ZnO NPs and reveals that the shape is quasi spherical and the average diameter is 26.6, 30.55 nm for ZnO and Ag-doped ZnO NPs respectively and doping with Ag makes no difference in the shape or size of ZnO NPs. The ZnO and Ag-doped ZnO NPs morphology were studied from SEM pictures in Figure 3, where we can notice that the ZnO nanoparticles looks uniform and have a semispherical shape (Figure3 (A)) and presence of Ag in Ag-doped ZnO sample doesn't make any change in the morphology in compared with ZnO sample which contains mainly pure ZnO as shown in Figure 3 (B).

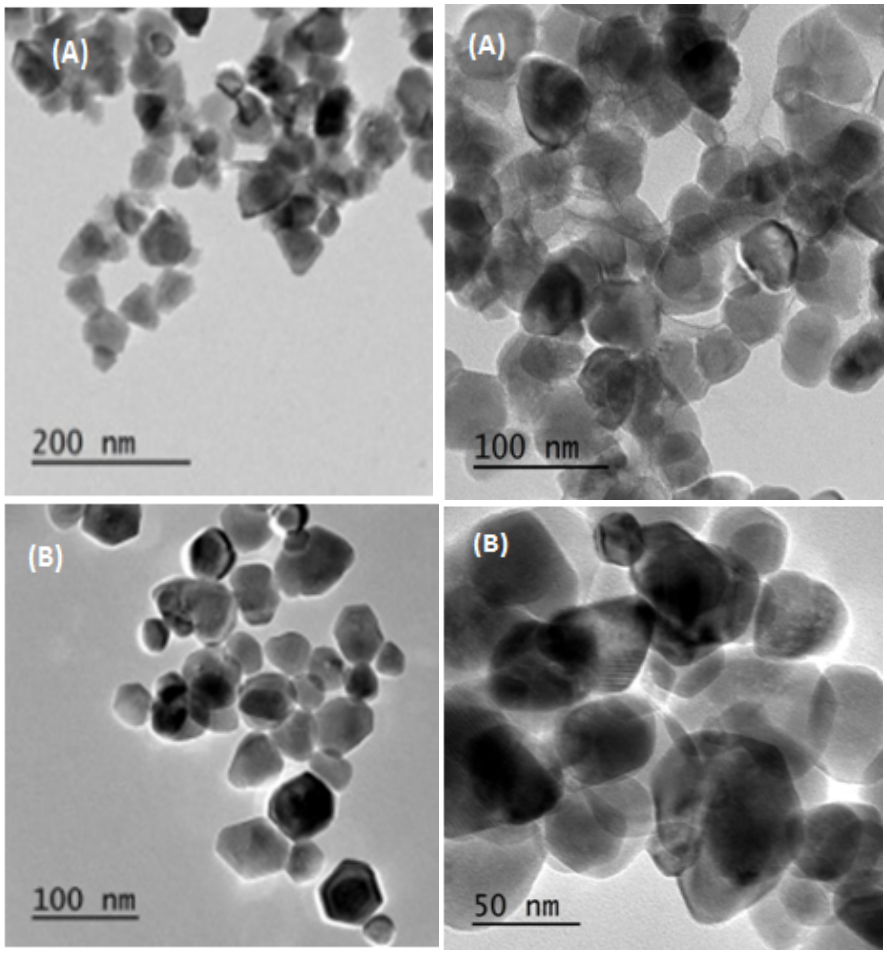

Figure 2 : The TEM images of (A) ZnO and (B) Ag-doped ZnO.

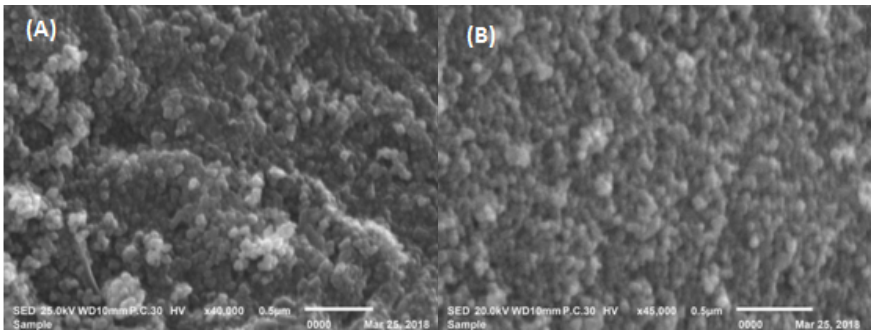

Figure 3 : The SEM images of (a) ZnO and (b) Ag-doped ZnO NPs.

SEM/EDX spectrum of the two samples is shown in Figure 4 which clearly indicates that ZnO sample is composed mainly of Zn and O, while Ag-doped ZnO sample contains Ag beside Zn and O.

The room temperature absorption spectra of ZnO and Ag-doped ZnO NPs solution in the UV and visible range are shown in Figure 5. The ZnO spectrum showed no absorption peaks above its fundamental absorption edge (around 400 nm). However the absorption spectra of Ag-doped ZnO shows an extra absorption peak in the visible light region, which is originated from the localized surface plasmon resonance of Ag NPs loaded on the surface of ZnO [29, 39].

The formation of ZnO and Ag-doped ZnO NPs were further confirmed by FT-IR spectral analysis in the range of 400 to 4000 cm^{-1} at room temperature, which is shown in Figure 6. Sharp peak was observed at~460 cm^{-1}, which can attributed to Zn-O stretching vibration mode. Peak at ~3400 is attributed to O-H stretching of surface adsorbed water molecule. The peaks at ~1560 and 1400 cm^{-1} are due to the symmetric and asymmetric bending modes of C=O bonds, respectively, while peaks at ~2850 and 2900 cm^{-1} are attributed to symmetric and asymmetric C-H stretching bonds respectively. There is no bands of silver in Ag-doped ZnO FT-IR spectrum, only that of ZnO, indicating there is no chemical bonding between silver and ZnO [40].

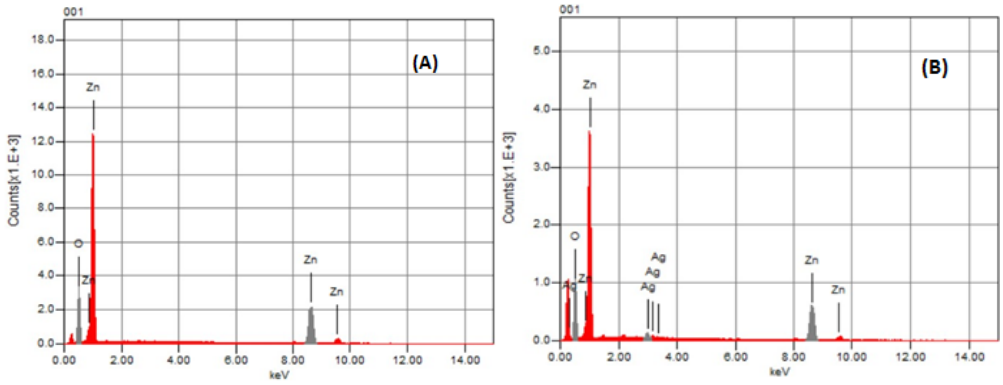

Figure 4 : SEM/EDX spectrum of (A)ZnO and (B) Ag-doped ZnO.

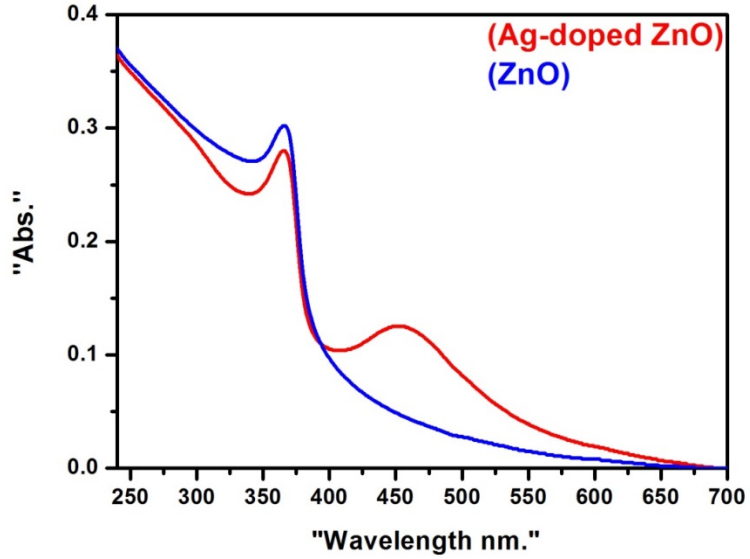

Figure 5 : UV-visible spectrum (ZnO) and (Ag-doped ZnO) NPs.

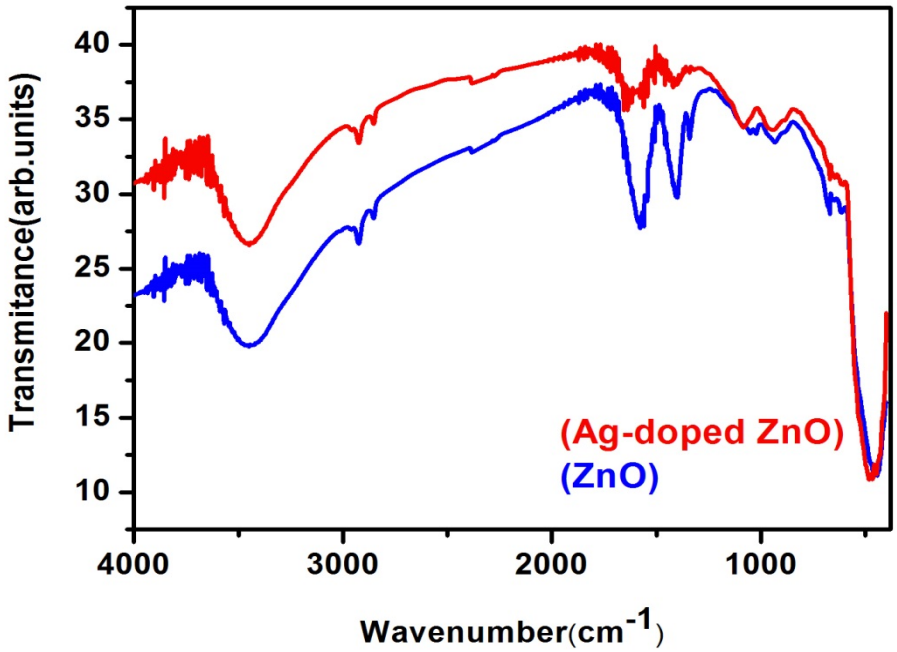

Figure 6: FTIR spectrum of (ZnO) and (Ag-doped ZnO) NPs.

3.2. Parameters effecting on photocatalytic activity

3.2.1. Effect of ZnO initial concentration

Study photocatalyst concentration effect on the photocatalytic degradation process is important for the cost and to achieve effective degradation of imidacloprid. To study this effect, solutions of ZnO with varied concentrations (25, 50, 100, 150, 200, 250) mg/L were vigorously stirred to make a homogenous solution, then 10 ml of each solution was added to 10 ml of imidacloprid solution (7 mg/L). The total solution was stirred in the dark for a few minutes to make an adsorption of imidacloprid on the surface of ZnO, then the solution was exposed to UV lamp for intervals time. A plot of % degradation rate of imidacloprid for various catalyst concentrations versus time was plotted Figure 7 which shows an increase in the degradation rate with increase in the ZnO initial concentration up to 50 mg/L and this increment can be attributed to increase of the number of active sites on the ZnO surface which in turn increase the number of hydroxyl and super oxide radicals [41]. A negative effect is observed when the ZnO concentration increase above 50 mg/L which may be resulted from a) agglomeration of ZnO particles causes a decrement in the specific surface area of adsorbent and b) number of photons reaching at the adsorbent active sites decreases due to screening effect by excess catalyst [42]. The photodegradation of imidacloprid is reported to follow a pseudo first-order model [43, 44], and the degradation rate constant (k) was (0.005, 0.007, 0.006, 0.005, 0.004, 0.003) for (25, 50, 100, 150, 200, 250) mg/L of ZnO NPs respectively.

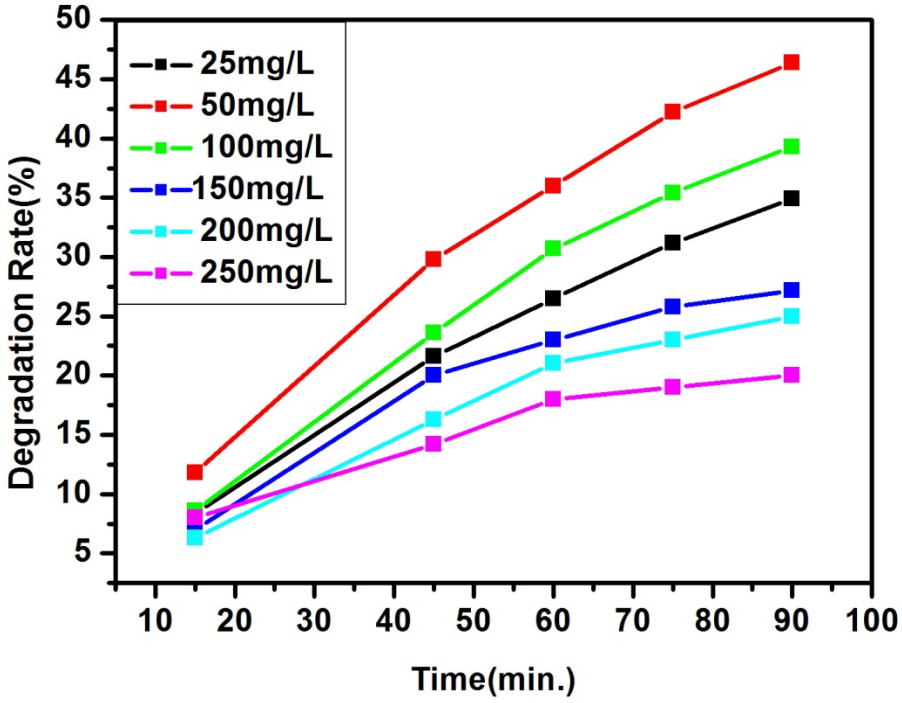

Figure 7 : Effect of ZnO concentration on photocatalytic degradation rate of imidacloprid.

3.2.2. Effect of imidacloprid initial concentration

The effect of initial concentration of imidacloprid on the overall rate of degradation was studied by varying the initial concentration over a wide range keeping all other parameters constant. Figure 8 shows that the rate of degradation which is related to the formation of OH radicals, that is the critical species in the degradation process, increases with increase in imidacloprid concentration up to 5.5 mg/L, but above this optimal concentration the rate decreases due to: a) insufficient quantity of OH radicals, as the formation of OH radicals is constant for a given amount of the catalyst b) the high concentration of imidacloprid may decrease the path length of photon entering the solution and may absorb significant amount of UV light rather than the catalyst [45-50].

3.2.3. Reaction temperature effect

The effect of reaction temperature on the imidacloprid degradation rate was studied by varying the temperature over a wide range (25, 30, 35, 40, 45 ^{o}C) keeping all other parameters constant. Figure 9 shows that with the imidacloprid degradation rate increases as the temperature increases up to 35^{o}C and this can be attributed to that

increase in temperature leads to: a) free radical generation resulted from bubble formation in the solution, b) helps to overcome the recombination of electro-hole pair and c) could enhance the imidacloprid oxidation reaction at the interface. A negative effect is observed above 35^{o}C and this may be resulted from that increase in temperature may decrease the absorbability of imidacloprid on ZnO surface which in turn will weaken the direct hole oxidation on the ZnO Photocatalyst surface [51].

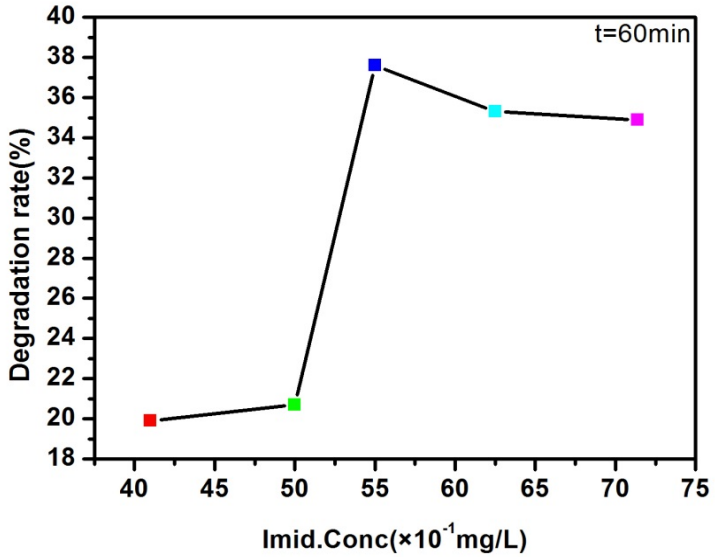

Figure 8 : Effect of imidacloprid initial concentration on its photocatalytic degradation rate.

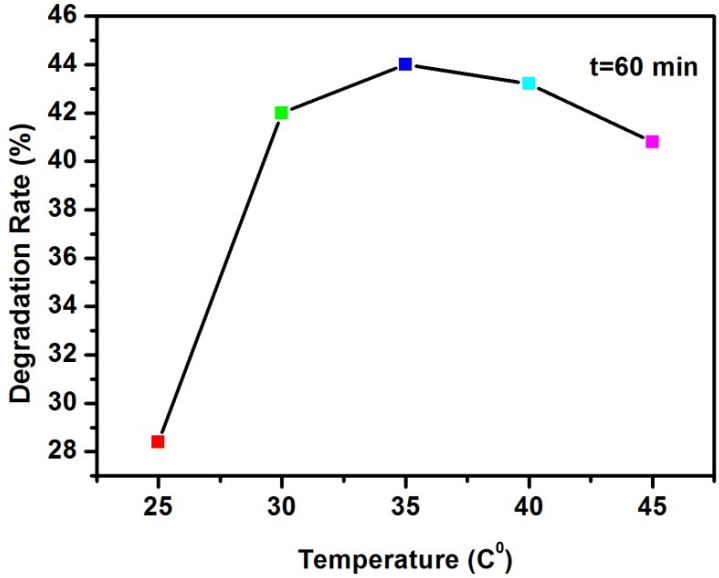

Figure 9: Effect of reaction temperatureon photocatalytic degradation rate of imidacloprid.

3.2.4. Solution initial pH effect

The pH effect, on organic compounds photo-degradation, is related to the acid-base equilibrium stability, which governs the catalyst surface chemistry in water. The pH of zero point charge (pH_{zpc}) for zinc oxide is approximately 9.0, above this value, the zinc oxide surface is negatively charged, whereas at pH lower than 9.0, the surface is positively charged. As shown in Figure10 the imidacloprid degradation rate increases as the pH increases and this can be attributed to that increase in pH may enhance a) electrostatic attraction between imidacloprid which have the strong electron withdrawing NO_2 group that increases the electropholecity of the azomethine carbon of nitroguanidine functional group [52] and ZnO NPs surface which is negatively charged when the pH of the solution is above its pH_{pzc} and this electrostatic attraction in turn increases the adsorption of imidacloprid molecule on the surface of ZnO NPs b) enhance the formation of OH radical and this in turn enhance the photoxidation process.

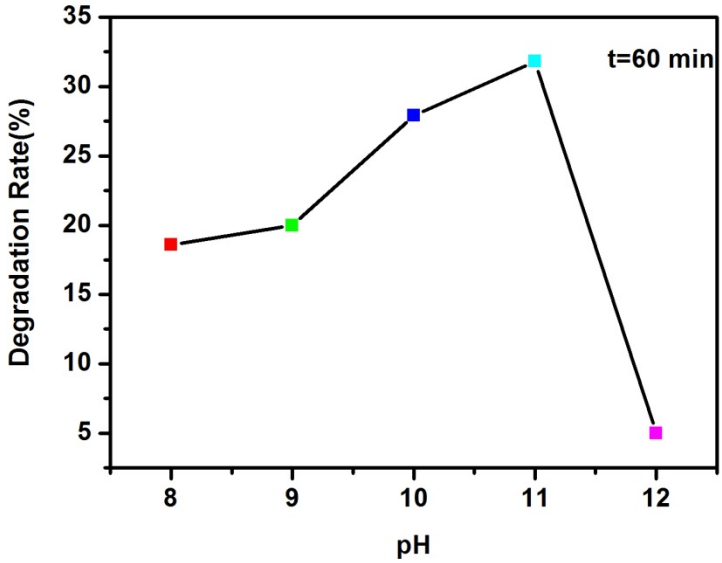

Figure 10 : Effect of pH on photocatalytic degradation rate of imidacloprid.

At very high pH the degradation is decreased this may be due to a) the resulting repulsion between the OH ions and the negatively charged surface of ZnO NPs b) excess adsorption of imidacloprid molecules on ZnO surface may impede the formation of OH radicals.

3.2.5. Effect of Ag doping

Figure11 shows the rate of photocatalytic degradation of imidacloprid catalyzed by both ZnO and Ag-doped ZnO NPs and the degradation rate constant (k) was (0.007 and 0.01) for ZnO and Ag-doped ZnO respectively. There is an enhancement, but it is somewhat slight. This enhancement is probably attributed to the more effective electron-hole separation of the Ag-doped ZnO NPs and this is due to that Ag NPs acting as an electron sink, can reduce the recombination of photoinduced electrons and holes and prolonged the lifetime of the electron hole pairs [25, 53]. Slightness can be attributed to the too high amount of silver in Ag-doped ZnO sample which was dark gray colored [34].

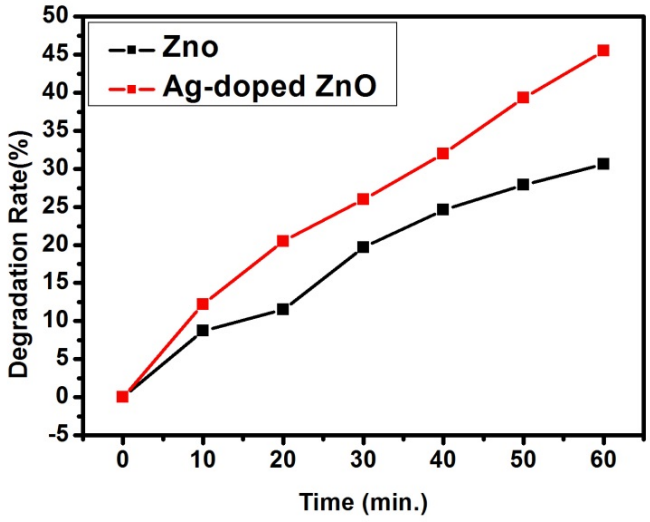

Figure 11: Rate of imidacloprid photocatalytic degradation catalyzed by (ZnO) and (Ag-doped ZnO) NPs.

Conclusion

According to this study, it can be concluded that there is an optimum value for each parameter at which ZnO NPs have the highest activity on imidacloprid photo degradation. For ZnO load it was 50 mg/L, 5.5 mg/L for imidacloprid initial concentration, 35^{o}C for reaction temperature and it is 11 for the pH value. Silver doping on the ZnO surface may enhance the imidacloprid photo degradation.

Acknowledgement-The authors gratefully acknowledge the University of Kafrelshikh for its support in this research.

References

1. A. O. Al-Jasser, King Saud University-Engineering Sciences. 23 (2011) 1.
2. S. Meli, M. Porto, A. Belligno, S. A. Bufo, A. Mazzatura, A. Scopa, Science of the Total Environment. 285 (2002) 69.
3. P. Dion, Soil biology and agriculture in the tropics, Springer, ISBN: 9783642050763 (2010).
4. Z. Filip, S. Kanazawa, J. Berthelin, Plant Nutrition and Soil Science. 163 (2000) 143.
5. F. M. Kiziloglu, M. Turan, U. Sahin, I. Angin, O. Anapali, M. Okuroglu, Plant Nutrition and Soil Science. 170 (2007) 166.
6. A. Libutti , G. Gatta, A. Gagliardi , P. Vergine , A. Pollice , L. Beneduce, G. Disciglio, E. Tarantino, Agricultural Water Management. 196 (2018) 1.
7. L. R. Beuchat, Food Protection. 59 (1996) 204.
8. J. Gatica, E. Cytryn, Environmental Science and Pollution Research 20 (2013) 3529.
9. M. P. T. Pham, J. W. Castle, J. H. Rodgers, Applied Water Science. 1 (2011) 85.
10. R. E. Sjogren, Water, Air, and Soil Pollution. 75 (1994) 389.
11. R. Tauxe, H. Kruse, C. Hedberg, M. Potter, J. Madden, K. Wachsmuth, Food Protection. 60 (1997) 1400.
12. A. El-Saharty, I. A. Hassan, Australian Journal of Basic and Applied Sciences. 8 (2014) 434.
13. M. N. Chong, B. Jin, C.W.K. Chow, C. Saint, Water Research. 44 (2010) 2997.
14. S.S. Turkar, D.B. Bharti, G.S. Gaikwad, Chemical and Pharmaceutical Research. 3 (2011) 58**.**
15. S. Baruah, S. K. Pal, J. Dutta, Nanoscience and Nanotechnology-Asia. 2 (2012) 90**.**
16. I. K. Konstantinou, T. A. Albanis, Applied Catalysis B: Environmental. 42 (2003) 319.
17. G. L. Hornyak, H.F. Tibbals, J. Dutta, J. J. Moore. "Introduction to nanoscience and nanotechnology, CRC press,ISBN: 9781420047790 (2008).
18. E. Bacaksiz, M. Parlak, M. Tomakin, A. Özçelik, M. Karakız, M. Altunbaş, Alloys and Compounds. 466 (2008) 447.
19. J. Wang, J. Cao, B. Fang, P. Lu, Sh. Deng, H. Wang, Materials Letters. 59 (2005) 1405.
20. A. Kołodziejczak-Radzimska, T. Jesionowski, Materials. 7 (2014) 2833.
21. H. H. Mohamed, D.W. Bahnemann, Applied Catalysis B: Environmental. 128 (2012) 91.
22. M. El-Kemary, H. El-Shamy, I. El-Mehasseb, Luminescence. 130 (2010) 2327.
23. A. L. Linsebigler, G. Lu, J. T. Yates , Chemical Reviews. 95 (1995) 735.
24. T.J. Whang, M.T. Hsieh, H.H. Chen, Applied Surface Science. 258 (2012) 2796.
25. M. El-Kemary,Y. Abdel-Moneam,M. Madkour,I. El-Mehasseb, Luminescence. 131 (2011) 570.
26. P. Christopher, H. Xin, S. Linic, Nature Chemistry. 3 (2011) 467.
27. C. Hu, T. Peng, X. Hu, Y. Nie, X. Zhou, J. Qu, H. He, The American Chemical Society. 132 (2010) 857.
28. X. Z. Lin, X. Teng, H. Yang, Langmuir. 19 (2003) 10081.
29. S. Linic, P. Christopher, D. B. Ingram, Nature Materials. 10 (2011) 911.
30. Y. Lu, G. L. Liu, L. P. Lee, Nano Letters. 5 (2005) 5.
31. X. Yan,X. Wang,W. Gu,M.M. Wu, Y. Yan,B.Hu,G. Che,D. Han,J. Yang,W. Fan,W. Shi, Applied Catalysis B: Environmental. 164 (2015) 297.
32. X. Zhou, G. Liu, J. Yu, W. Fan, Materials Chemistry. 22 (2012) 21337.
33. X. Zhang, Y. Lim Chen, R. Liu, D. Ping Tsai, Reports on Progress in Physics. 76 (2013) 046401.
34. Z. Papp, Chemija. 25 (2014) 1.
35. N. Simon-Delso, V. Amaral-Rogers, L. P. Belzunces, J. M. Bonmatin, M. Chagnon, C. Downs, L. Furlan, D. W. Gibbons, C. Giorio, V. Girolami, D. Goulson, D. P. Kreutzweiser, C. H. Krupke, M. Liess, E. Long, M. McField, P. Mineau, E. A. D. Mitchell, C. A. Morrissey, D. A. Noome, L. Pisa, J. Settele, J. D. Stark, A. Tapparo, H. Van Dyck, J. Van Praagh, J. P. Van der Sluijs, P. R. Whitehorn, M. Wiemers, Environ Sci Pollut Res Int. 22 (2015) 5.
36. P. M. Aneesh, K. A.Vanaja, M. K. Jayaraj, International Society for Optics and Photonics, Nanophotonic Materials IV. 6639 (2007) 66390J1.

37. T. Alammar, A. Mudring, Materials Science. 44 (2009) 3218.
38. L. Duan, B. Lin, W. Zhang, Sh. Zhong, Z. Fu, Applied Physics Letters. 88 (2006) 232110.
39. P. Wang, B. Huang, X. Zhang, X. Qin, H. Jin, Y. Dai, Z. Wang, J. Wei, J. Zhan, Sh. Wang, J. Wang, M. Whangbo, Chemistry-A European Journal. 15 (2009) 1821.
40. R. Georgekutty, M. K. Seery, S. C. Pillai, Physical Chemistry C. 112 (2008) 13563.
41. M.V. Shankar, K. K. Cheralathan, B. Arabindoo, M. Palanichamy, V. Murugesan, Molecular Catalysis A: Chemical. 223 (2004) 195.
42. S. Rabindranathan, S. Devipriya, S. Yesodharan, Hazardous Materials. 102 (2003) 217.
43. S. Kurwadkar, A. Evans, D. Dewinne, P. White, F. Mitchell, Environmental Toxicology and Chemistry. 35 (2015) 1718.
44. A. Derbalah, M. Sunday, R. Chidya, W. Jadoon, H. Sakugawa, Water Health 17 (2019) 254.
45. A.Akbari Shorgoli, M. Shokri, Chemical Engineering Communications. 204 (2017) 1061.
46. S. Ahmed,M. G. Rasul,R. Brown,M. A. Hashib, Environmental Management. 92 (2011) 311.
47. S. Ahmed, M. G. Rasul, W. N. Martens, R. Brown, M. A. Hashib, Water, Air, & Soil Pollution. 215 (2011) 3.
48. G. Balasubramanian, D. D Dionysiou, M. T Suidan, I. Baudin, J. M. Laîné, Applied Catalysis B: Environmental. 47 (2004) 73.
49. C.H. Chiou, C.Y. Wu, R. S. Juang, Chemical Engineering. 139 (2008) 322.
50. A. R. Khataee, M. N. Pons, O. Zahraa, Hazardous Materials. 168 (2009) 451.
51. K. Hashimoto, H. Irie, A. Fujishima, Japanese Journal of Applied Physics. 44 (2005) 8269.
52. V. Guzsvány, J. Csanádi, F. Gaál, Acta Chimica Slovenica. 53 (2006) 52.
53. H.A. Rafaie, N.A.M. Safian, R.M. Nor, Y.M. Amin, Malaysian Journal of Analytical Sciences. 22 (2018) 435.

(2019) ; http://www.jmaterenvironsci.com